Published OnlineFirst December 14, 2018; DOI: 10.1158/1541-7786.MCR-18-0530

Signal Transduction and Functional Imaging

Molecular Cancer Research

CCL2 Is a Vascular Permeability Factor Inducing CCR2-Dependent Endothelial Retraction during Lung Metastasis

Marko Roblek[1], Darya Protsyuk[1], Paul F. Becker[2], Cristina Stefanescu[1], Christian Gorzelanny[3], Jesus F. Glaus Garzon[1], Lucia Knopfova[4,5], Mathias Heikenwalder[2,6], Bruno Luckow[7], Stefan W. Schneider[3], and Lubor Borsig[1]

Abstract

Increased levels of the chemokine CCL2 in cancer patients are associated with poor prognosis. Experimental evidence suggests that CCL2 correlates with inflammatory monocyte recruitment and induction of vascular activation, but the functionality remains open. Here, we show that endothelial Ccr2 facilitates pulmonary metastasis using an endothelial-specific Ccr2-deficient mouse model (Ccr2^{ec}KO). Similar levels of circulating monocytes and equal leukocyte recruitment to metastatic lesions of Ccr2^{ec}KO and *Ccr2$^{fl/fl}$* littermates were observed. The absence of endothelial Ccr2 strongly reduced pulmonary metastasis, while the primary tumor growth was unaffected. Despite a comparable cytokine milieu in Ccr2^{ec}KO and *Ccr2$^{fl/fl}$* littermates the absence of vascular permeability induction was observed only in Ccr2^{ec}KO mice. CCL2 stimulation of pulmonary endothelial cells resulted in increased phosphorylation of MLC2, endothelial cell retraction, and vascular leakiness that was blocked by an addition of a CCR2 inhibitor. These data demonstrate that endothelial CCR2 expression is required for tumor cell extravasation and pulmonary metastasis.

Implications: The findings provide mechanistic insight into how CCL2–CCR2 signaling in endothelial cells promotes their activation through myosin light chain phosphorylation, resulting in endothelial retraction and enhanced tumor cell migration and metastasis.

Introduction

Metastasis is the main reason for cancer-related fatalities. Hematogenous metastasis is a multistep process depending on interactions of disseminated tumor cells with the microenvironment (e.g., platelets and leukocytes) and ultimately with the endothelium in distant organs (1, 2). Tumor cell migration through vascular barriers is promoted by the recruitment of monocytic cells that contribute to formation of a metastatic niche (3–5). Proinflammatory chemokines, particularly CCL2, were linked to the accumulation of CCR2-expressing inflammatory monocytes during metastasis (6–9). High levels of proinflammatory chemokines, e.g., CCL2 and CCL5, in circulation are associated with poor prognosis for cancer patients (reviewed in ref. 10). Therefore, many studies explored the genetic and pharmacologic inhibition of the CCL2–CCR2 axis as a mean to impair monocyte recruitment to metastatic sites. Whereas CCL2 clearly potentiates monocyte recruitment *in vitro* (11), other tumor- or stroma-derived chemokines (e.g., CCL3, CCL5) may contribute to this process *in vivo* (4, 10). Similarly, inflammatory monocytes, defined as Ly6C^{hi} and CCR2^{+} cells, express several chemokine receptors, e.g., CCR1, which can facilitate chemokine-driven monocyte recruitment to sites of inflammation or tumorigenesis (12). For instance, CCR2 was not required for inflammatory monocyte recruitment in an acute inflammation model (13, 14).

The CCL2–CCR2 chemokine/chemokine receptor axis is required for the egress of inflammatory monocytes from the bone marrow to the circulation during homeostasis and inflammation (13, 14). Thus, systemic Ccr2 deficiency or a treatment with CCL2 neutralizing agents resulted in reduced circulating monocyte numbers (8, 13). In addition, increased circulating serum levels of Ccl2 resulted in reduced responsiveness of blood cells to other chemokines (15). Similarly, anti-CCL2 antibody treatment of rheumatoid arthritis patients results in higher CCL2 serum levels and worsening of the disease symptoms (16).

There is accumulating evidence that CCR2 on stromal cells, particularly on endothelium, has a physiologic role during inflammation (17, 18). Activation of brain endothelial CCR2 by

[1]Institute of Physiology, University of Zurich and Zurich Center for Integrative Human Physiology, Zurich, Switzerland. [2]Institute of Virology, Technische Universität München/Helmholtz Zentrum Munich, Munich, Germany. [3]Department of Dermatology and Venerology, University Hospital Hamburg-Eppendorf, Hamburg, Germany. [4]Department of Experimental Biology, Faculty of Science, Masaryk University, Brno, Czech Republic. [5]International Clinical Research Center, Center for Biological and Cellular Engineering, St. Anne's University Hospital, Brno, Czech Republic. [6]German Cancer Research Centre (DKFZ), Division of Chronic Inflammation and Cancer, Heidelberg, Germany. [7]Medizinische Klinik und Poliklinik IV, Klinikum der Universität München, LMU München, Munich, Germany.

Note: Supplementary data for this article are available at Molecular Cancer Research Online (http://mcr.aacrjournals.org/).

M. Roblek and D. Protsyuk contributed equally to this article.

Current address for M. Roblek: Institute of Science and Technology (IST) Austria, A-3400 Klosterneuburg, Austria.

Corresponding Author: Lubor Borsig, University of Zurich, Winterthurerstrasse 190, 8057 Zurich, Switzerland. Phone: 41-44-635-5134; Fax: 41-44-635-6814; E-mail: lborsig@access.uzh.ch

doi: 10.1158/1541-7786.MCR-18-0530

Published OnlineFirst December 14, 2018; DOI: 10.1158/1541-7786.MCR-18-0530

CCL2 induced vascular leakiness (18) and regulated macrophage transendothelial migration (TEM; ref. 17). Furthermore, CCR2-mediated endothelial activation was linked to tumor-associated angiogenesis (19). Although tumor cell–derived CCL2 expression is associated with enhanced metastasis, the analysis of metastatic lungs revealed that recruited monocytes and endothelial cells significantly contribute to an increased pool of CCL2 at metastatic sites (5). Recently, endothelial activation by CCL2 was directly linked to tumor cell–induced lung vascular permeability (9, 20); however, the underlying mechanism remains unclear.

Endothelial retraction is an essential step in metastasis both during intravasation and extravasation. Phosphorylation of VE-cadherin has been shown to be essential for initiation of TEM of leukocytes (21) and also tumor cells (5). Recent data show that VE-cadherin rearrangement in endothelial cells is associated with enhanced phosphorylation of myosin light chain 2 (MLC2) during angiogenesis (22). In addition, inhibition of VE-cadherin rearrangement, which is associated with reduced MLC2 phosphorylation, in endothelial cells maintains endothelial barrier function during inflammation (23).

Tumor-derived chemokines actively shape the tumor microenvironment and directly affect various cell types both at primary and at metastatic sites (10, 24). Here we show that CCR2 signaling in lung endothelial cells induces cytoskeletal rearrangement resulting in enhanced vascular permeability required for monocyte-assisted tumor cell TEM and metastatic initiation.

Materials and Methods

Cell culture

Primary lung endothelial cells were isolated by immunomagnetic selection using anti-CD31 antibody and cultivated as described previously (9). Bone marrow monocytes were isolated from femur and tibia followed by magnetic anti-CD115 purification as described previously (5). Mouse carcinoma cell lines MC-38GFP and LLC1.1 were grown as described (5). The immortalized mouse brain endothelial cell line bEnd.3 (from ATCC) was grown in DMEM/10% FCS supplemented with 1× NEAA and 1 mmol/L Na pyruvate.

Mice

All animal experiments were performed according to the guidelines of the Swiss Animal Protection Law and approved by the Veterinary Office of Kanton Zurich. C57BL/6J (wt) mice as well as systemic Ccr2-deficient mice, B6.129S4-Ccr2$^{<tm1Ifc/J>}$, were purchased from The Jackson Laboratory. *VE-cad-Cre/Ccr2$^{fl/fl}$* mouse (hereafter Ccr2^{ec}KO mouse) was generated by breeding the *Ccr2$^{fl/fl}$* mouse (ref. 25; obtained from M. Pasparakis) with the VE-cadherin-Cre mouse, B6.FVB-Tg(Cdh5-cre)7Mlia/J (ref. 26; The Jackson Laboratory) in C57BL/6J background. *Ccr2$^{fl/fl}$* and Ccr2^{ec}KO littermates were used for all experiments. Mice expressing a VE-cadherin–EGFP fusion protein through a DNA construct knocked into the Cdh5 locus (27) were obtained from D. Vestweber.

Transmigration assay

Primary lung endothelial cells (3×10^4) were seeded on gelatin-coated 24-well transwell inserts with 8-μm pores (BD) and allowed to grow to confluency. Endothelial cells were preincubated with the following inhibitors: 50 μmol/L RS504393 (CCR2), 50 μmol/L 2-APB (IP_3-gated Ca^+ channels), 10 μmol/L BAPTA-AM (chelating intracellular $Ca2^+$), 1 μmol/L ML-7 (MLCK), 5 μmol/L H-1152 (ROCK2), and 2.5 μmol/L blebbistatin (myosin II ATPase) for 2 hours in RPMI1640/10% FCS medium (all inhibitors were purchased from Tocris). The first 4 inhibitors were used according to the manufacturer's recommendations (Tocris); for H-1152 and blebbistatin, we used concentrations as previously published (28). Upon removal of inhibitors from the endothelial cells MC-38GFP cells (2×10^4) were added in the presence or absence of CD115$^+$ monocytes (1×10^5) in RPMI1640/3% FCS. Transmigration was induced with RPMI1640/10% FCS in the lower chamber and terminated after 16 hours. Alternatively, MC-38GFP cells (2×10^4) were added to the upper insert with or without rhCCL2 (1 μg/mL; kindly provided by A. Kungl, University of Graz). The number of transmigrated MC-38GFP cells was counted using a Zeiss AxioVision microscope ($n \geq 3$).

Transendothelial electrical resistance

Transendothelial electrical resistance (TEER) was measured using Electric Cell-Substrate Impedance Sensing (ECIS) as reported (29). When a constant impedance of the endothelial layer was detected (24 hours after seeding), rhCCL2 (10 μg/mL) was added to cells. Impedance was measured every 48 seconds (ECIS-zeta system; Applied BioPhysics Inc.) for 22 hours at a frequency of 4,000 Hz, while cells were continuously maintained in a humidified atmosphere at 37°C and 5% CO_2. Statistical significance was calculated by an unpaired *t* test.

Preparation of cell lysates

Primary lung microvascular cells or bEnd.3 cells were stimulated with 40 ng/mL IL1β (R&D Systems) for 2 hours in RPMI1640/10% FCS and washed with PBS prior to the addition of CCL2; 100 ng/mL (R&D Systems) in RPMI1640/10% FCS for indicated times. CCR2 was blocked with 50 μmol/L RS504393 inhibitor during IL1β and CCL2 stimulation. Cells were scraped-off the plates in ice-cold 1× PBS, centrifuged for 5 minutes and lysed in 100 μL cell lysis buffer (20 mmol/L Tris pH 7.5, 150 mmol/L NaCl, 1 mmol/L EDTA, and 1% Triton X-100) supplemented with phosphatase inhibitor cocktail 3 (Sigma) and complete protease inhibitor cocktail (Roche) for 20 minutes on ice. After centrifugation, cell lysates were stored at −80°C.

Western blot

Cell lysate (20 μg) was separated on a 15% SDS-PAGE gel, transferred to a nitrocellulose membrane Protran 0.45 NC (GE Healthcare) and blocked with 5% BSA/TBS-T (1% Tween 20) for 1 hour at RT. Primary antibodies: rabbit antiphosphoMLC2 (Ser19; Cell Signaling Technology), anti–β-catenin (Cell Signaling Technology), anti–VE-cadherin (Abcam), and mouse anti–β-actin (Sigma) were incubated overnight at 4°C. After washing with TBS-T (3×), the membrane was incubated with a secondary antibody: HRP-linked-anti-rabbit IgG (Cell Signaling Technology) or anti-mouse IgG, HRP-linked (Cell Signaling Technology) for 1 hour at RT. After washing with TBS-T (3×), the membrane was developed with ECL West Dura solution (Thermo Fisher Scientific), and chemiluminescent signal was detected using Hyperfilm ECL (GE Healthcare).

Immunoprecipitation

The endothelial cell line bEnd.3 was stimulated with 40 ng/mL IL1β (R&D Systems) for 2 hours in RPMI1640/10% FCS. After

Published OnlineFirst December 14, 2018; DOI: 10.1158/1541-7786.MCR-18-0530

washing with PBS, cells were incubated with 1 μg/mL rhCCL2 in RPMI/10% FCS for 1 hour. Cell lysates were prepared as mentioned above, and β-catenin was immunoprecipitated with anti–β-catenin antibody overnight at 4°C in the presence of protein G beads (GE Healthcare). Beads were washed (3×) with the lysis buffer, boiled in Laemmli buffer and separated on a 7.5% SDS-PAGE gel, followed by Western blotting.

Cell sorting of endothelial cells

Lungs of mice were perfused with PBS followed by digestion with Collagenase A and Collagenase D (2 mg/mL each, Roche) in RPMI1640/2% FCS for 1 hour at 37°C. The digested tissue was filtered through a 100-μm cell strainer, RBC lysed, and filtered again through a 40-μm cell strainer. Resuspended cells were incubated with an F_c block (eBioscience) for 10 minutes in FACS buffer (PBS/10 mmol/L EDTA, 2% FCS), followed by incubation with antibodies: CD45-PB, CD11b-APC-Cy7, CD31-PE-Cy7, Ly6C-FITC, and Ly6G-PerCP-Cy5.5 (all from BD) for 30 minutes on ice. After washing, endothelial cells ($CD45^-CD11b^-CD31^+$) were sorted on a FACSAria III 5L (BD).

RNA preparation, cDNA generation, and qPCR

RNeasy Mini Kit (Qiagen) was used for RNA isolation from cells *in vitro*, and TRI Reagent (Sigma) was used for RNA isolation from perfused lungs. cDNA was prepared from 250 ng RNA using the Omniscript RT Kit (Qiagen) according to the manufacturer's instructions. Real-time PCR was performed using SYBR Green JumpStart Taq ReadyMix kit (Sigma) with gene-specific intron-spanning primers (Supplementary Table S1) on the Mx3000P qPCR cycler (Agilent). Cycle conditions: 95°C for 30 seconds, 60°C for 30 seconds, 72°C for 30 seconds. GAPDH was used as an internal control.

Flow cytometry of peripheral blood and lungs

Blood was mixed with PBS/5 mmol/L EDTA and spun down. Lung tissue was digested as described above. After RBC lysis with PharmLyse (BD), resuspended leukocytes were incubated with F_c block (eBioscience) in FACS buffer for 10 minutes and followed by staining with the following antibodies: CD45-APC-Cy7, CD11b-PE-Cy7, Ly6C-FITC, Ly6G-PerCP-Cy5.5, CD45-PerCP-Cy5.5, CD3-APC-Cy7, CD4-FITC, CD8-PE-Cy7, CD11b-BV510, CD19-APC, NK1.1-PerCP-Cy5.5, CD45-PB, anti-CD11b-APC-Cy7, anti-Ly6C-APC (all from BD), and CD146-PerCP-Cy5.5 (BioLegend) for 30 minutes on ice. For staining of CCR2, we used MC-21 antibody (30), followed by goat-anti-rat-PE antibodies (BD). Data were acquired with a FACSCanto (BD), in some cases with CountBright absolute counting beads (Life Technologies), and analyzed by FlowJo software (TreeStar).

Metastasis models

Lewis lung carcinoma cells LLC1.1 (300,000 cells) were subcutaneously (s.c.) injected into mice. Primary tumor was removed after 14 days, and mice were terminated 4 weeks after s.c. injection. Perfused lungs were imaged, and metastatic foci were counted. The primary tumor and the metastatic lungs were fixed and paraffin sections were prepared. MC-38GFP colon cancer cells (300,000) or LLC1.1 cells (150,000) were intravenously injected (i.v.). MC-38GFP–injected mice were terminated after 4 weeks, and LLC1.1-injected mice after 2 weeks. Perfused lungs were imaged, and metastatic foci were counted. The lungs were fixed and paraffin sections histologically evaluated.

Evans Blue assay

Ccr2$^{fl/fl}$ and Ccr2^{ec}KO mice were s.c. injected with 300,000 LLC1.1 cells. After 14 days, 2 mg/mL of Evans Blue solution (Sigma) was i.v. injected, and the lungs were perfused with PBS 30 minutes later and analyzed (9).

Histology and IHC

Tissue paraffin sections (2 μm) were stained with hematoxylin/eosin or the following antibodies: F4/80 (Serotec), Ly6G (BD), CD31 (Abcam), CD3 (NeoMarkers), B220 (BD), Ki67 (NeoMarkers), and cleaved caspase-3 (BD). Staining was performed on a NEXES immune-histochemistry robot (Ventana Instruments) using an IVIEW DAB Detection Kit (Ventana Instruments) or on a Bond MAX (Leica). Images were digitized with a SCN400 slide scanner (Leica) and analyzed using Tissue IA image analysis software in a double-blind manner (Slidepath, Leica). Tissue sections were stained simultaneously for each antigen and the signal-to-noise cutoff was manually adjusted for each antibody staining. This cutoff was applied to all samples within one staining group, and positive signal (above the cutoff) is displayed as a percentage of the total area analyzed.

Cytokine analysis

Cytokines in lung tissue lysates (200 μg) were measured with the ProcartaPlex Mouse Panel 1 (26-plex) kit and VEGF (10 μg lysate) with the Mouse VEGF-A Platinum ELISA kit (both eBioscience).

Statistical analysis

Statistical analysis was performed with the GraphPad Prism software (version 6.03). All data are presented as mean ± SEM and were analyzed by ANOVA with the *post hoc* Bonferroni multiple comparison test. Analysis of 2 groups was performed with the Mann–Whitney test unless stated otherwise.

Results

Characterization of mice with endothelial-specific deletion of Ccr2

To define the function of endothelial CCR2 in controlling tumor cell extravasation, we made a mouse with an endothelial cell–specific deletion of Ccr2. For this purpose, the VE-cadherin-Cre mouse (26) was bred with the *Ccr2*$^{fl/fl}$ mouse (25) to generate the *VE-cad-Cre/Ccr2*$^{fl/fl}$ mouse (hereafter Ccr2^{ec}KO mouse). The cell-specific deletion of Ccr2 was confirmed by qPCR of sorted pulmonary endothelial cells (Supplementary Fig. S1A). We observed the same levels of circulating inflammatory ($Ly6C^{hi}$) and patrolling ($Ly6C^{int}$) monocytes in *Ccr2*$^{fl/fl}$ and Ccr2^{ec}KO mice (Supplementary Fig. S1B). In contrast, reduced numbers of $Ly6C^{hi}$ monocytes were detected in *Ccr2*$^{-/-}$ mice as reported previously (9, 13). Other circulating leukocyte subsets were not altered between *Ccr2*$^{fl/fl}$ and Ccr2^{ec}KO littermates. Unchanged amount of CCR2 expression was detected on inflammatory monocytes ($Ly6C^{hi}$) in the peripheral blood of Ccr2^{ec}KO and *Ccr2*$^{fl/fl}$ mice (Supplementary Fig. S1C, left). Because VE-cadherin expression has also been detected in myeloid $CD11b^+$ cells (26), we analyzed the expression of CCR2 in knock-in mice expressing

Published OnlineFirst December 14, 2018; DOI: 10.1158/1541-7786.MCR-18-0530

VE-cadherin-GFP from the VE-cadherin genetic locus Cdh5-EGFP (27). We observed no GFP expression in circulating Ly6C^{hi} cells (Supplementary Fig. S1C, right). Next, we analyzed the endothelial progenitor cells (CD45$^-$CD31$^+$CD146$^+$) of the lungs (31). A reduced CCR2 expression was detected on endothelial progenitor cells from Ccr2^{ec}KO mice when compared with *Ccr2$^{fl/fl}$* mice (Fig. 1A). Importantly, the level of CCR2 expression on inflammatory monocytes in Ccr2^{ec}KO mice remained unaffected (Supplementary Fig. S1C). Overall, these data indicate that endothelial *Ccr2* deletion does not interfere with the homeostasis of inflammatory monocytes.

Primary tumor growth is not altered by the absence of endothelial Ccr2

To assess the role of endothelial Ccr2 during tumorigenesis, mice were s.c. injected with Lewis lung carcinoma (LLC1.1) cells and spontaneous metastases to the lungs were determined. The tumor weight of dissected primary tumors was similar in all mouse genotypes after 14 days (Fig. 1B). Histologic analysis of primary tumors revealed no difference in the number of recruited F4/80$^+$ macrophages, Ly6G$^+$ neutrophils, CD3$^+$ T cells, and B220$^+$ B cells between *Ccr2$^{fl/fl}$* and Ccr2^{ec}KO mice (Fig. 1C; Supplementary Fig. S1D). The number of proliferating cells

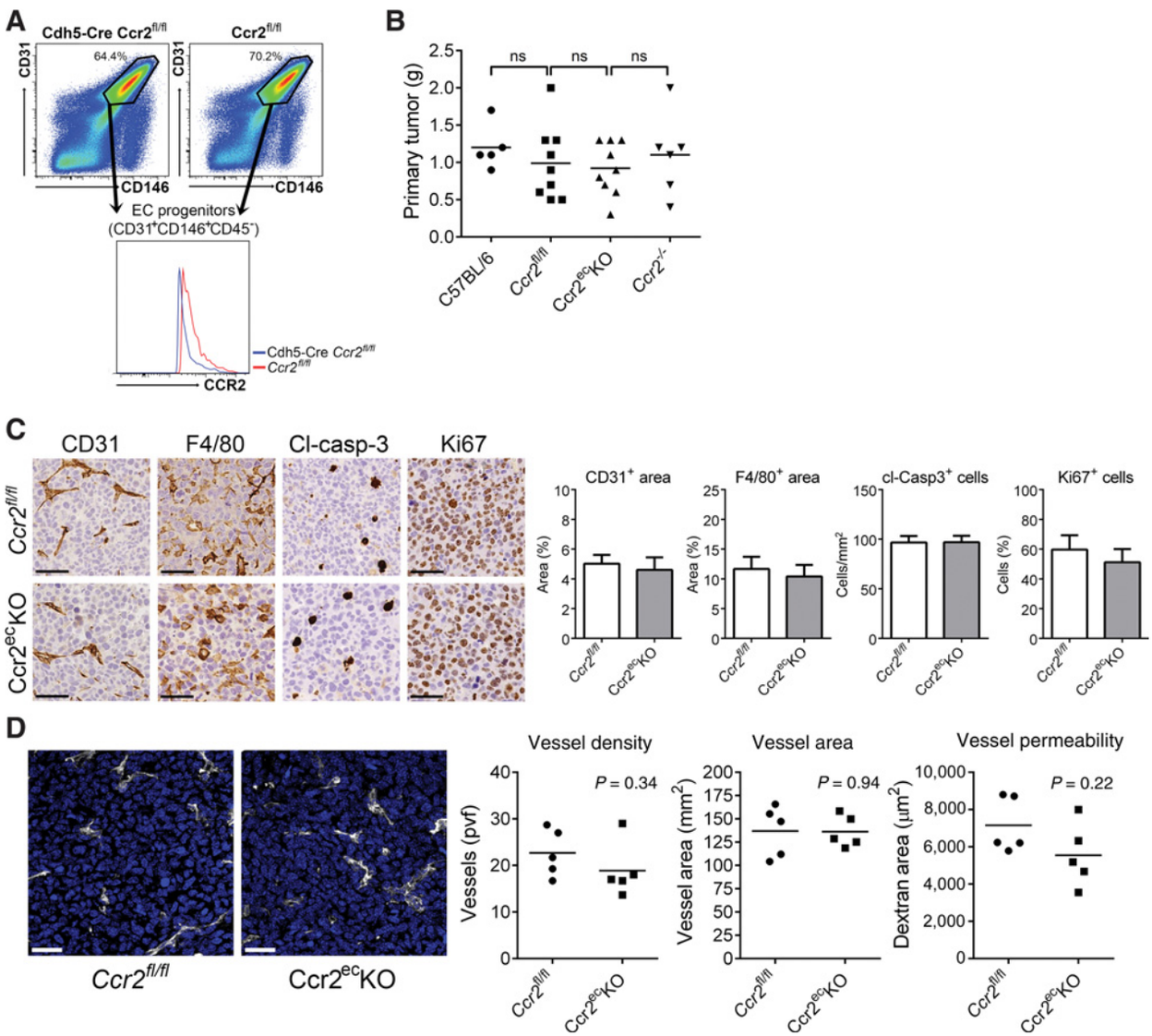

Figure 1.

Primary tumor growth was not affected by the endothelial deficiency of CCR2. **A,** Analysis of endothelial progenitor cells (CD31$^+$CD146$^+$CD45$^-$) in the lungs of naïve Ccr2^{ec}KO mice and *Ccr2$^{fl/fl}$* mice. **B,** Weight of primary subcutaneous LLC1.1 tumors at the time of resection (14 days after implantation); ns, not significant. **C,** Representative images of primary tumors stained with CD31, F4/80, cl-Casp3, and Ki67 Abs together with histologic analysis, respectively. Bar, 50 μm. **D,** Representative images of primary tumors from Ccr2^{ec}KO and *Ccr2$^{fl/fl}$* mice, respectively, stained with anti-CD31 (white) to analyze vascular density (nuclear staining with DAPI, blue). The analysis of vessel density and vessel area revealed no difference between mice of both genotypes. Vessel permeability in tumors was determined using intravenous injection of dextran-FITC 1 hour prior to termination. Cryosections of the tumors were analyzed for the dextran-FITC. Bar, 30 μm.

Published OnlineFirst December 14, 2018; DOI: 10.1158/1541-7786.MCR-18-0530

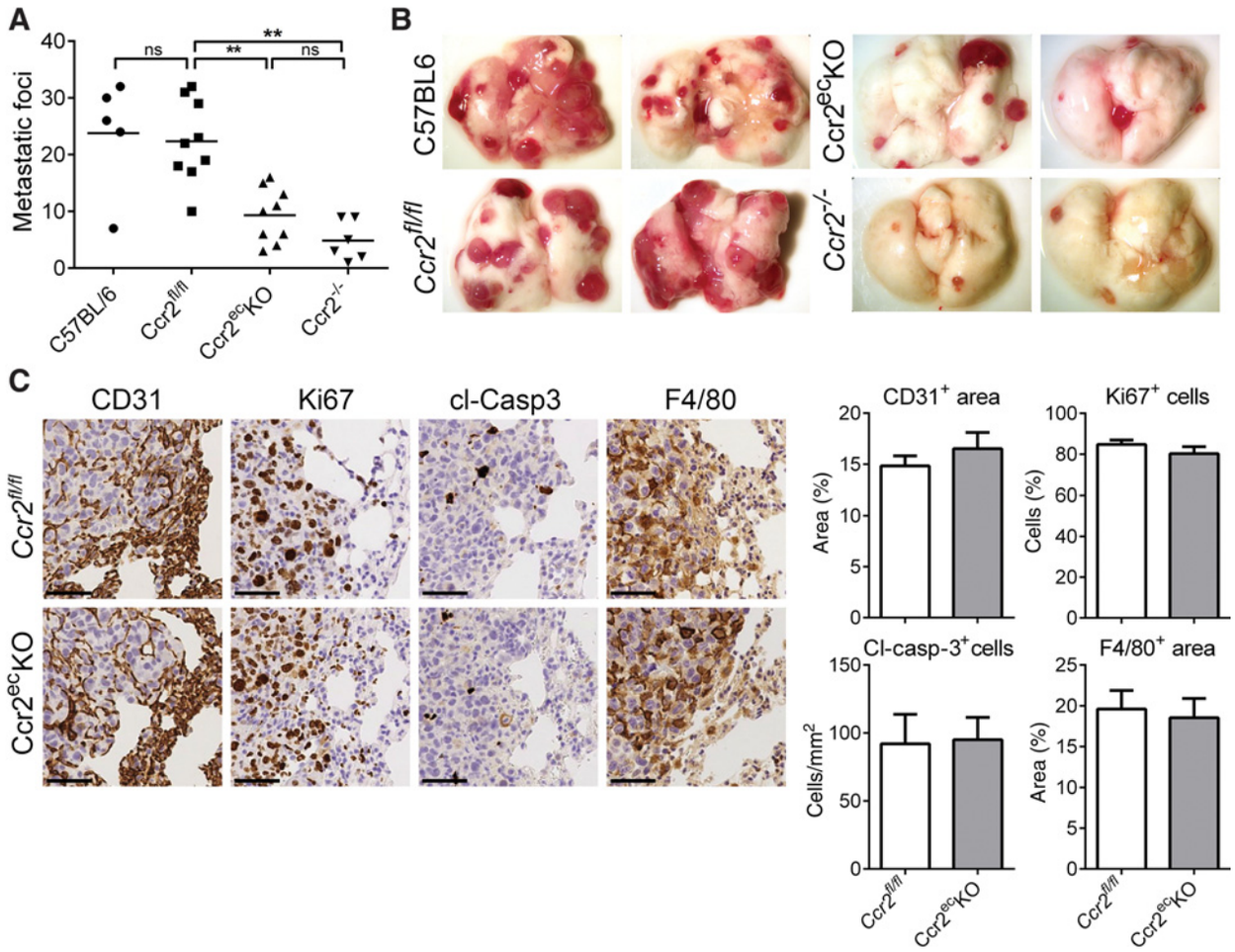

Figure 2.

Endothelial Ccr2 is required for lung metastasis. **A,** Spontaneous lung metastasis in C57BL/6, *Ccr2*$^{fl/fl}$, Ccr2^{ec}KO, and *Ccr2*$^{-/-}$ mice 28 days after subcutaneous injection of LLC1.1 cells. **, $P < 0.01$; ns, not significant. **B,** Representative images of lungs from mice analyzed in **A**. **C,** Representative images of pulmonary metastasis stained with anti-CD31 (vasculature) and anti-F4/80 (macrophages) antibodies. Proliferating cells (Ki67 staining) and apoptotic cells (cleaved caspase-3 staining; cl-Casp3) were evaluated. The edge of a metastatic lesion is presented. The histologic analysis of metastatic foci only was performed. Bar, 50 μm.

(Ki67$^+$ cells), apoptotic cells (cleaved-caspase3$^+$ cells) in primary tumors was identical between both mouse genotypes. To assess the effect of endothelial CCR2 deficiency on tumor angiogenesis, we analyzed tumor vessel density, vessel area and vessel permeability (Fig. 1D). We observed no differences in any of the endothelial parameters in primary tumors irrespective of endothelial CCR2 expression, suggesting that overall endothelial physiology, including tumor angiogenesis, is not affected by endothelial CCR2.

The absence of endothelial Ccr2 attenuates lung metastases

After the primary tumor removal, mice were terminated at 28 days after tumor cell injection (p.i.) and spontaneous lung metastases analyzed (Fig. 2A and B). We observed a significant reduction of metastases in Ccr2^{ec}KO mice, when compared with *Ccr2*$^{fl/fl}$ littermates. Although the number of metastases in *Ccr2*$^{fl/fl}$ mice was comparable with wild-type (C57BL/6J) mice, the reduced metastases detected in Ccr2^{ec}KO mice were comparable with *Ccr2*$^{-/-}$ mice. Histologic analysis of lung metastases revealed no difference in the number of infiltrating macrophages (F4/80$^+$ cells), neutrophils (Ly6G$^+$), T cells (CD3$^+$), and B cells (B220$^+$) between lungs from Ccr2^{ec}KO or *Ccr2*$^{fl/fl}$ mice (Fig. 2C; Supplementary Fig. S2A). Importantly, we found similar vascular density (CD31$^+$ area) within the metastatic foci in both mouse genotypes, indicating no difference in angiogenesis (Fig. 2C). The number of proliferating cells (Ki67$^+$ cells) and apoptotic cells (cleaved-caspase3$^+$ cells) was equal in the metastatic foci of Ccr2^{ec}KO and *Ccr2*$^{fl/fl}$ mice.

We further tested the endothelial CCR2 requirement for metastases using intravenous injection of LLC1.1 and colon carcinoma cells MC-38GFP. Experimental metastases of both cell types were significantly reduced in Ccr2^{ec}KO mice when compared with *Ccr2*$^{fl/fl}$ littermates (Supplementary Fig. S2B and S2C). These results show that the absence of endothelial Ccr2 strongly attenuates the generation of pulmonary metastases.

Published OnlineFirst December 14, 2018; DOI: 10.1158/1541-7786.MCR-18-0530

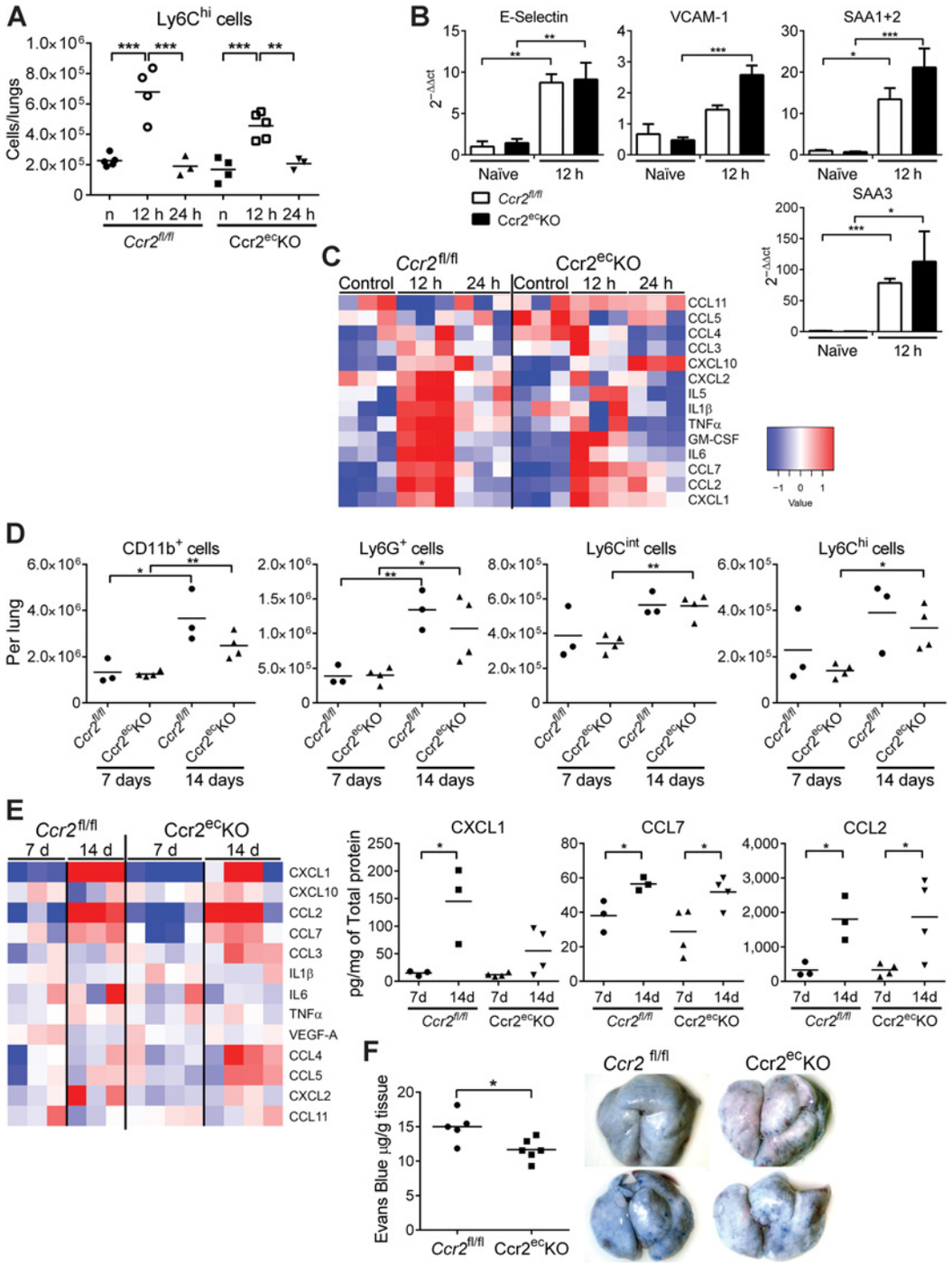

Figure 3.

Initiation of the premetastatic niche is not impaired in Ccr2^{ec}KO mice. **A,** Flow cytometry analysis of inflammatory monocytes (CD45$^+$CD11b$^+$Ly6G$^-$Ly6C^{hi}) recruited to the lungs at 12 and 24 hours after i.v. MC-38GFP injection of *Ccr2$^{fl/fl}$* and Ccr2^{ec}KO mice. Untreated naïve mice (*n*) were used as controls. **B,** Endothelial cells (CD45$^-$CD11b$^-$CD31$^+$) sorted from lungs of *Ccr2$^{fl/fl}$* and Ccr2^{ec}KO mice 12 hours after i.v. MC-38GFP injection or untreated (naïve) mice were analyzed for the expression levels of E-selectin, VCAM-1, SAA1+2, and SAA3 ($n = 3$–6). **C,** Amounts of cytokines in perfused lung homogenates of *Ccr2$^{fl/fl}$* and Ccr2^{ec}KO mice at 12 and 24 hours after i.v. MC-38GFP injection. Untreated mice (control) were used as controls. **D,** Flow cytometry analysis of myeloid cells (CD45$^+$CD11b$^+$), granulocytes (CD45$^+$CD11b$^+$Ly6G$^+$), Ly6C^{int} monocytes (CD45$^+$CD11b$^+$LyG$^-$Ly6C^{int}), and inflammatory monocytes (CD45$^+$CD11b$^+$Ly6G$^-$Ly6C^{hi}) recruited to lungs of mice s.c. injected with LLC1.1 cells after 7 and 14 days. **E,** Amounts of cytokines detected in lung homogenates of mice s.c. injected with LLC1.1 cells after 7 and 14 days. **F,** Lung vascular permeability assay of *Ccr2$^{fl/fl}$* and Ccr2^{ec}KO mice 14 days after s.c. injection of LLC cells, including representative macroscopic images. Statistical significance in **B, D, E,** and **F** was assessed using an unpaired *t* test; *, $P < 0.05$; **, $P < 0.01$; ***, $P < 0.001$.

Published OnlineFirst December 14, 2018; DOI: 10.1158/1541-7786.MCR-18-0530

Formation of the metastatic niche in lungs remains unaltered in Ccr2^{ec}KO mice

To test whether the endothelial Ccr2-deficiency influences the metastatic niche formation, we analyzed lungs from mice that were intravenously injected with MC-38GFP cells. Previous analysis has shown that LLC1.1 and MC-38GFP cells induce similar responses during lung metastasis (5). We observed increased recruitment of inflammatory monocytes (Ly6C^{hi} cells) at 12 hours p.i. in both *Ccr2$^{fl/fl}$* and Ccr2^{ec}KO littermates (Fig. 3A), which returned to normal levels 24 hours p.i., as reported previously for wt mice (9). The numbers and the recruitment kinetics of myeloid cells (CD11b^{+}), granulocytes (Ly6G^{+}), and Ly6C^{int} monocytes were similar between the 2 genotypes (Supplementary Fig. S3A).

The analysis of tumor cell–induced endothelial activation revealed an increase in E-selectin and VCAM-1 mRNA expression 12 hours p.i. that was similar in both *Ccr2$^{fl/fl}$* and Ccr2^{ec}KO littermates (Fig. 3B). Serum amyloid A3 (SAA3) and S100A8 have been associated with hyperpermeable regions in metastatic lungs (20). We observed a comparable increase in the serum amyloid A expressions (SAA1, SAA2, and SAA3) in sorted endothelial cells from lungs of *Ccr2$^{fl/fl}$* and Ccr2^{ec}KO littermates 12 hours p.i. (Fig. 3B). The cytokine analysis in the lungs of *Ccr2$^{fl/fl}$* and Ccr2^{ec}KO mice at 12 hours and 24 hours p.i. revealed similar kinetics of cytokine expression on protein levels (Fig. 3C). Chemokines (CXCL1, CCL2, CCL3, and CCL7) and cytokines (GM-CSF and IL6) associated with endothelial activation and monocyte recruitment/activation increased at 12 hours p.i. and returned to normal levels at 24 hours p.i. irrespective of a mouse genotype. Thus, the absence of endothelial Ccr2 has no apparent effect on leukocyte recruitment, cytokine milieu, or endothelial activation in naïve or metastatic lungs.

Increased vascular permeability is dependent on endothelial Ccr2 expression

To test whether the absence of endothelial Ccr2 affects the formation of a premetastatic niche, we analyzed lungs of mice s.c. injected with LLC1.1 cells at 7 and 14 days p.i. by flow cytometry. Increased recruitment of myeloid cells (CD11b^{+}), granulocytes (Ly6G^{+}), Ly6C^{int} monocytes, and inflammatory monocytes (Ly6C^{hi}) to the premetastatic lungs was detected at day 14 in both *Ccr2$^{fl/fl}$* and Ccr2^{ec}KO littermates (Fig. 3D). Lymphoid cell recruitment remained the same irrespective of a mouse genotype (Supplementary Fig. S3B). Similarly, increased amounts of myeloid cell subpopulations were detected in the peripheral blood at day 14, which correlated with the primary tumor growth progression (Supplementary Fig. S3C).

An increase in chemokines (e.g., CXCL1, CCL7, and CCL2) in premetastatic lungs was observed with tumor growth progression

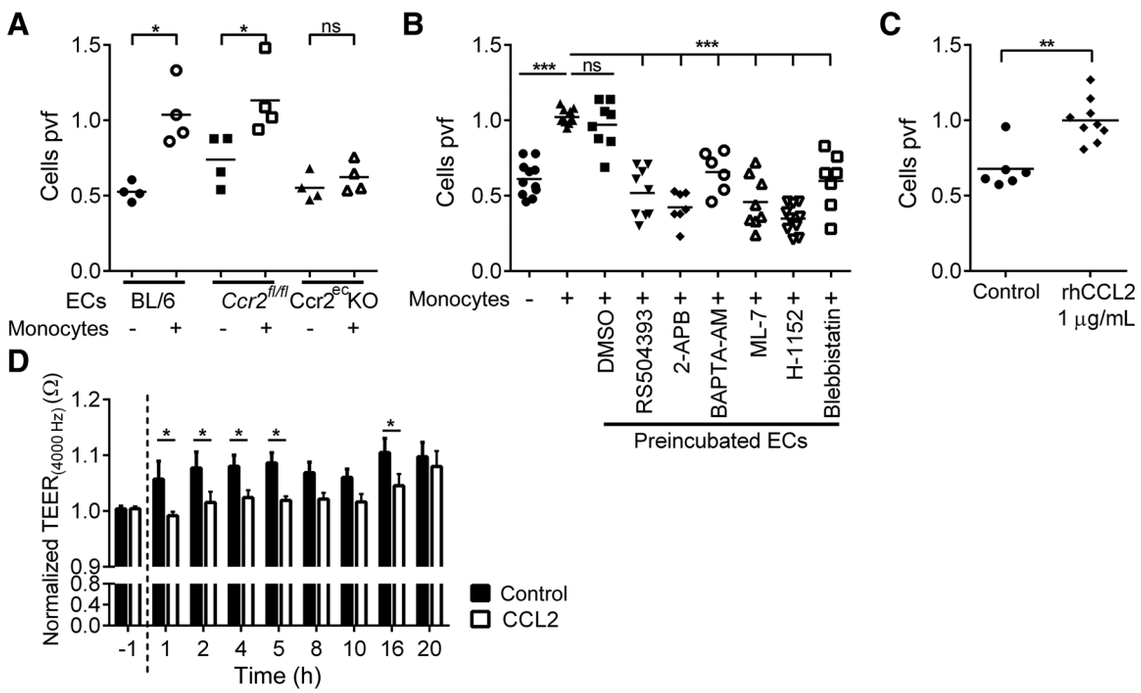

Figure 4.

CCL2 stimulation induces endothelial retraction and TEM of tumor cells. **A,** TEM of MC-38GFP cells through lung endothelial cells isolated from C57BL/6 wild-type (BL6), *Ccr2$^{fl/fl}$* and Ccr2^{ec}KO mice, either in the absence (−) or in the presence of CD115^{+} monocytes (+). The number of migrated tumor cells was counted per view field (pvf) and is normalized to the control (+ monocytes); ns; not significant; *, $P < 0.05$. **B,** TEM of MC-38GFP cells in the absence (−) or in the presence of CD115^{+} monocytes (+). Endothelial cells from C57BL/6 mice (EC) were pretreated with RS-504393 (50 μmol/L), 2-APB (50 μmol/L), BAPTA-AM (10 μmol/L), ML-7 (1 μmol/L), H-1152 (5 μmol/L), and blebbistatin (2.5 μmol/L) for 2 hours and washed out of the inhibitor prior to the addition of tumor cells ± monocytes. DMSO as a diluent of inhibitors was used as a control. Tumor cell migration was analyzed as described in **A**. ***, $P < 0.001$. **C,** TEM of MC-38GFP cells (without monocytes) only in the presence of rhCCL2 (1 μg/mL) compared with a control. **, $P < 0.01$. **D,** TEER measurement of primary lung endothelial cells upon stimulation with rhCCL2 (10 μg/mL). TEER values for rhCCL2-treated and control samples were normalized to 1 at the start of stimulation (0 hours). Black bars, control; open bars, CCL2 treated; $n = 4$; *, $P < 0.05$; other time points showed no significant differences.

Published OnlineFirst December 14, 2018; DOI: 10.1158/1541-7786.MCR-18-0530

but did not differ between *Ccr2*$^{fl/fl}$ and Ccr2^{ec}KO mice (Fig. 3E). Despite reduced metastasis in the absence of endothelial Ccr2, no changes in the metastatic niche of the lungs were observed. Thus, we tested whether the lung vasculature is altered in tumor-bearing mice at 14 days. We detected small, but significant, reduction in the vascular permeability of Ccr2^{ec}KO mice when compared with *Ccr2*$^{fl/fl}$ littermates (Fig. 3F). These findings indicate that the endothelial Ccr2 deficiency prevents induction of vascular permeability, which is required for lung metastasis.

CCL2 induces loosening of endothelial junctions and the contraction of endothelial cells

Reduced vascular permeability has been previously linked to attenuated tumor cell extravasation and metastasis (5, 9). Thus, we tested the capacity of tumor cells to migrate through pulmonary endothelial cells derived from Ccr2^{ec}KO and *Ccr2*$^{fl/fl}$ mice. TEM of tumor cells through wild-type endothelial cells was significantly potentiated by the addition of monocytes (Fig. 4A), as described previously (9). However, TEM of tumor cells was potentiated by monocytes only through endothelial cells derived from *Ccr2*$^{fl/fl}$ but not from Ccr2^{ec}KO mice (Fig. 4A). To identify the signaling cascade facilitating the CCL2-induced vascular permeability, we targeted the G-protein–coupled receptor pathway that is required for the actin–myosin complex activation (Fig. 4B). Interestingly, the preincubation of endothelial cells with inhibitors of CCR2 (RS504393), IP_3-receptor (2-APB), intracellular Ca^{2+} (BAPTA-AM), myosin light chain kinase MLCK (ML-7), Rho-associated kinase ROCK (H-1152), and myosin II ATPase (Blebbistatin) significantly reduced TEM of tumor cells. Of note, endothelial cells pretreated with RS504393, ML-7, or H-1152 also showed impaired TEM of 4T1 breast cancer cells (Supplementary Fig. S4A). These data indicate that inhibition of endothelial retraction attenuates monocyte-assisted TEM of tumor cells. Importantly, an addition of recombinant CCL2 also increased TEM of MC-38GFP cells in the absence of monocytes (Fig. 4C). Because MC-38GFP cells do not express Ccr2 (32), we tested the hypothesis that CCL2 activates endothelial CCR2, which results in endothelial retraction. We measured TEER of primary pulmonary endothelial cells after stimulation with CCL2. TEER of the endothelial monolayer decreased upon CCL2 stimulation compared with the control (Fig. 4D; Supplementary Fig. S4B), confirming that CCL2 stimulation triggers endothelial retraction.

Activation of actin–myosin contraction is required for cell retraction and depends on phosphorylation of myosin light chain 2 (pMLC2; ref. 33). Stimulation of endothelial cells with CCL2 resulted in accumulation of pMLC2 (Fig. 5A). The analysis of an endothelial cell line bEnd.3 showed that CCL2 activation induced the accumulation of pMLC2 1 to 2 hours after stimulation (Fig. 5B). We observed no changes in total MLC2 expression but only an increase in MLC2 phosphorylation (Supplementary

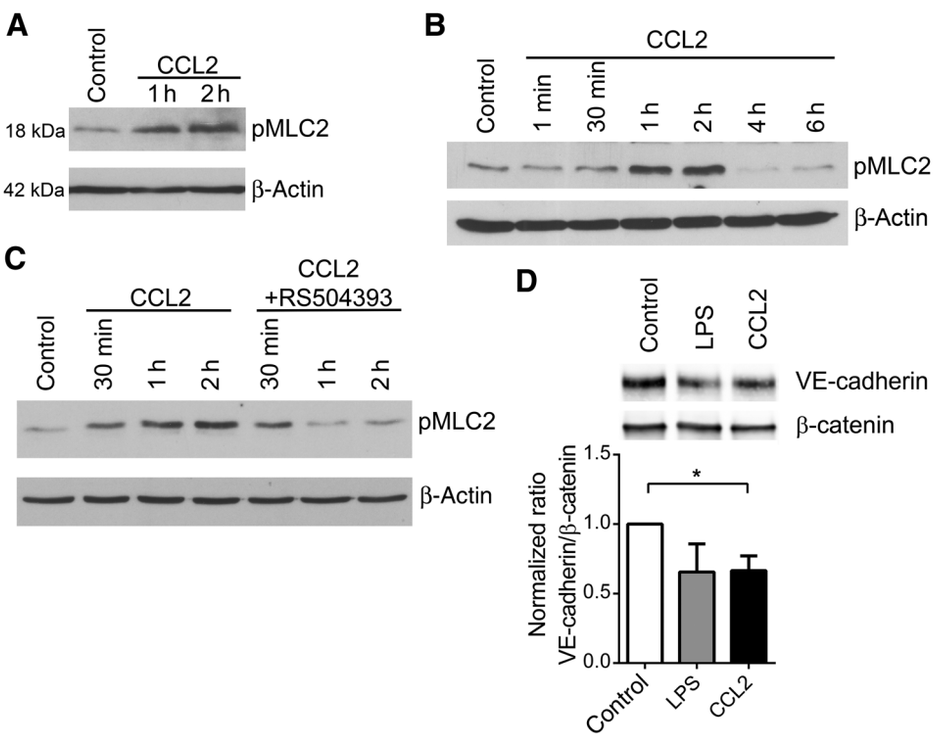

Figure 5.

CCL2 stimulation of endothelial cells induces phosphorylation of myosin light chain 2 and loosening of endothelial barrier. **A,** Immune detection of phosphorylated MLC2 (pMLC2) in the lysates of primary pulmonary endothelial cells after stimulation with CCL2 (100 ng/mL) for 1 and 2 hours. Per lane, 20 μg of protein lysate was loaded; β-actin served as a loading control. **B,** Detection of pMLC2 in bEnd.3 endothelial cells after stimulation with CCL2 (100 ng/mL). β-Actin served as a loading control. **C,** Immune-detection of pMLC2 in lysates of bEnd.3 endothelial cells stimulated with CCL2 (100 ng/mL) for 30 minutes, 1 hour, and 2 hours in the absence or presence of the CCR2 inhibitor RS504393 (50 μmol/L). Per lane 20 μg of protein lysate was loaded; β-actin served as a loading control. **D,** Immunoprecipitation of β-catenin and detection of coimmunepreciptated VE-cadherin in bEnd.3 cell lysates stimulated with rhCCL2 (1 μg/mL) for 1 hours. Quantification of immune-precipitated VE-cadherin in ratio to β-catenin (bottom) $n = 4$, *, $P < 0.05$.

Published OnlineFirst December 14, 2018; DOI: 10.1158/1541-7786.MCR-18-0530

Fig. S5A). To prove that endothelial pMLC2 accumulation is driven by CCL2 stimulation, we treated bEnd.3 cells with a CCR2 inhibitor that resulted in diminished phosphorylation of MLC2 (Fig. 5C). Loosening of the endothelial barrier is caused by the dissociation of VE-cadherin/β-catenin complex (34). CCL2 stimulation of endothelial cells resulted in dissociation of the VE-cadherin/β-catenin complex (Fig. 5D), hence confirming a direct effect of CCL2 on endothelial barrier function. CCL2-activated bEnd.3 cells also showed reduced VE-cadherin colocalization with β-catenin (Supplementary Fig. S5B–S5C), thereby complementing the immunoprecipitation data (Fig. 5D). These data provide evidence that CCL2-driven activation of endothelial CCR2 results in the cytoskeletal rearrangement and loosening of the endothelial cell junctions and thereby facilitates an efficient TEM of tumor cells.

Discussion

Dissemination of tumor cells during metastasis is promoted by platelet- and monocyte-assisted extravasation from the circulation (3, 5, 9, 35). Particularly, the chemokine/chemokine receptor axis CCL2–CCR2 appears to be involved in several steps during metastasis, including leukocyte recruitment, angiogenesis, immune suppression, and cancer cell extravasation (6–9, 35). Because the systemic inhibition of CCR2/CCL2 interferes with the egress of inflammatory monocytes from the bone marrow (13, 36), the observed reduced recruitment of monocytes to metastatic sites is rather a consequence of reduced numbers of circulating Ly6C^{hi} cells. To dissect the contribution of endothelial Ccr2 from the Ccr2-dependent monocyte recruitment to metastasis, we generated an endothelial cell–specific Ccr2 deletion mouse model (Ccr2^{ec}KO mice). In this model, we observed no alteration in the numbers of circulating cells or in the recruitment of inflammatory monocytes to metastatic lungs. Nevertheless, a significant attenuation of metastasis was observed in Ccr2^{ec}KO mice when compared with control littermates. Taken together, these findings suggest that the local activation of endothelial Ccr2 is essential for tumor cell extravasation during lung metastasis.

Endothelial CCR2 has been linked to regulation of the blood–brain barrier vascular permeability during inflammation (18, 37) and to the regulation of angiogenesis (38, 39). Recently, we have shown that endothelial CCR2 promotes metastasis by facilitating tumor cell extravasation (9). In this report, we show that neither the primary tumor growth nor the tumor angiogenesis were affected by the absence of endothelial CCR2, which is agreement with previous findings that endothelial CCR2 expression has been observed only in the brain and the lungs (9, 38). Notably, the absence of endothelial Ccr2 did not alter the endothelial activation upon tumor cell challenge.

TEM of cells is a tightly regulated process that controls distribution of leukocytes throughout the organism (40). Induction of vascular permeability is essential for an efficient TEM of tumor cells (9, 20, 41). Enhanced vascular permeability in lungs was previously associated with a Ccr2-dependent increase of inflammatory permeability factors SAA1+2 and SAA3 (20). We observed similar cytokine and chemokine levels in the lungs of tumor-challenged mice of Ccr2^{ec}KO and *Ccr2*$^{fl/fl}$ genotypes. Although similar levels of permeability factors such as VEGF-A, SAA3, and CCL2 were detected in the lungs of Ccr2^{ec}KO and *Ccr2*$^{fl/fl}$ mice, we observed impaired induction of vascular permeability only in Ccr2^{ec}KO mice. These results demonstrate that endothelial CCR2 is the regulator of tumor cell–induced lung vascular permeability. Furthermore, TEER was decreased by CCL2 stimulation of endothelial cells, indicating the loosening and disassembly of endothelial intercellular junctions. Inhibition of CCR2 or the proteins regulating the endothelial actin–myosin cytoskeleton (MLCK, ROCKII, and myosin II) severely impaired tumor cell TEM *in vitro*. In endothelial cells, MLC2 phosphorylation represents the sole regulation of myosin II ATPase activity during inflammation or angiogenesis (22, 23, 42–44). Indeed, CCL2 stimulation of endothelial cells induced phosphorylation of MLC2, which could be blocked by a CCR2 inhibitor. Presented data provide evidence that CCR2-mediated endothelial activation induces disassembly of adherens junctions, thereby facilitating TEM of tumor cells.

In conclusion, we describe a mechanism how endothelial CCR2 regulates lung metastasis through the activation of the actin–myosin cytoskeleton using by an endothelial cell–specific Ccr2-deficient (Ccr2^{ec}KO) mouse model. Translation of CCR2 inhibition into clinical setting will require timely and spatially defined approach, due to the homeostatic function of CCL2–CCR2 signaling mediating the release of monocytes from the bone marrow (36). Systemic inhibition of CCL2 in mouse models led to reduction of breast cancer metastasis, however; cessation of a treatment resulted in accelerated tumor growth due to an enhanced release of monocytes from the bone marrow (8). Nevertheless, targeting of CCR2 inhibitors to the metastatic niche attenuated metastasis without any side effects (32, 45). Further progress in cell-specific targeting will show whether CCR2 targeting will be of therapeutic value.

Disclosure of Potential Conflicts of Interest

No potential conflicts of interest were disclosed.

Authors' Contributions

Conception and design: M. Roblek, M. Heikenwalder, L. Borsig
Development of methodology: M. Roblek, D. Protsyuk
Acquisition of data (provided animals, acquired and managed patients, provided facilities, etc.): M. Roblek, D. Protsyuk, C. Stefanescu, C. Gorzelanny, J.F. Glaus Garzon, L. Knopfova, B. Luckow, S.W. Schneider, L. Borsig
Analysis and interpretation of data (e.g., statistical analysis, biostatistics, computational analysis): M. Roblek, D. Protsyuk, P.F. Becker, C. Stefanescu, J.F. Glaus Garzon, M. Heikenwalder, S.W. Schneider, L. Borsig
Writing, review, and/or revision of the manuscript: M. Roblek, P.F. Becker, M. Heikenwalder, B. Luckow, L. Borsig
Study supervision: L. Borsig

Acknowledgments

This study was supported by the SNF grant #310030-173076 (L. Borsig). The authors acknowledge the assistance of the Center for Microscopy and Image Analysis, University of Zurich, for confocal microscopy experiments. M. Heikenwalder was supported by an ERC Consolidator grant (HepatoMetaboPath). We thank the group of Dr. D. Vestweber for providing the VE-Cad-EGFP mouse.

The costs of publication of this article were defrayed in part by the payment of page charges. This article must therefore be hereby marked *advertisement* in accordance with 18 U.S.C. Section 1734 solely to indicate this fact.

Received May 23, 2018; revised August 30, 2018; accepted December 4, 2018; published first December 14, 2018.

Published OnlineFirst December 14, 2018; DOI: 10.1158/1541-7786.MCR-18-0530

References

1. Labelle M, Hynes RO. The initial hours of metastasis: the importance of cooperative host-tumor cell interactions during hematogenous dissemination. Cancer Discov 2012;2:1091–9.
2. Quail DF, Joyce JA. Microenvironmental regulation of tumor progression and metastasis. Nat Med 2013;19:1423–37.
3. Qian B, Deng Y, Im JH, Muschel RJ, Zou Y, Li J, et al. A distinct macrophage population mediates metastatic breast cancer cell extravasation, establishment and growth. PLoS One 2009;4:e6562.
4. Kitamura T, Qian BZ, Pollard JW. Immune cell promotion of metastasis. Nat Rev Immunol 2015;15:73–86.
5. Hauselmann I, Roblek M, Protsyuk D, Huck V, Knopfova L, Grassle S, et al. Monocyte induction of E-selectin-mediated endothelial activation releases VE-cadherin junctions to promote tumor cell extravasation in the metastasis cascade. Cancer Res 2016;76:5302–12.
6. Lu X, Kang Y. Chemokine (C-C motif) ligand 2 engages CCR2+ stromal cells of monocytic origin to promote breast cancer metastasis to lung and bone. J Biol Chem 2009;284:29087–96.
7. Qian BZ, Li J, Zhang H, Kitamura T, Zhang J, Campion LR, et al. CCL2 recruits inflammatory monocytes to facilitate breast-tumour metastasis. Nature 2011;475:222–5.
8. Bonapace L, Coissieux MM, Wyckoff J, Mertz KD, Varga Z, Junt T, et al. Cessation of CCL2 inhibition accelerates breast cancer metastasis by promoting angiogenesis. Nature 2014;515:130–3.
9. Wolf MJ, Hoos A, Bauer J, Boettcher S, Knust M, Weber A, et al. Endothelial CCR2 signaling induced by colon carcinoma cells enables extravasation via the JAK2-Stat5 and p38MAPK pathway. Cancer Cell 2012;22:91–105.
10. Borsig L, Wolf MJ, Roblek M, Lorentzen A, Heikenwalder M. Inflammatory chemokines and metastasis-tracing the accessory. Oncogene 2014;33:3217–24.
11. Volpe S, Cameroni E, Moepps B, Thelen S, Apuzzo T, Thelen M. CCR2 acts as scavenger for CCL2 during monocyte chemotaxis. PLoS One 2012;7:e37208.
12. Shi C, Pamer EG. Monocyte recruitment during infection and inflammation. Nat Rev Immunol 2011;11:762–74.
13. Serbina NV, Pamer EG. Monocyte emigration from bone marrow during bacterial infection requires signals mediated by chemokine receptor CCR2. Nat Immunol 2006;7:311–7.
14. Shi C, Jia T, Mendez-Ferrer S, Hohl TM, Serbina NV, Lipuma L, et al. Bone marrow mesenchymal stem and progenitor cells induce monocyte emigration in response to circulating Toll-like receptor ligands. Immunity 2011;34:590–601.
15. Cardona AE, Sasse ME, Liu L, Cardona SM, Mizutani M, Savarin C, et al. Scavenging roles of chemokine receptors: chemokine receptor deficiency is associated with increased levels of ligand in circulation and tissues. Blood 2008;112:256–63.
16. Haringman JJ, Gerlag DM, Smeets TJ, Baeten D, van den Bosch F, Bresnihan B, et al. A randomized controlled trial with an anti-CCL2 (anti-monocyte chemotactic protein 1) monoclonal antibody in patients with rheumatoid arthritis. Arthritis Rheum 2006;54:2387–92.
17. Dzenko KA, Song L, Ge S, Kuziel WA, Pachter JS. CCR2 expression by brain microvascular endothelial cells is critical for macrophage transendothelial migration in response to CCL2. Microvasc Res 2005;70:53–64.
18. Stamatovic SM, Keep RF, Kunkel SL, Andjelkovic AV. Potential role of MCP-1 in endothelial cell tight junction 'opening': signaling via Rho and Rho kinase. J Cell Sci 2003;116:4615–28.
19. Salcedo R, Ponce ML, Young HA, Wasserman K, Ward JM, Kleinman HK, et al. Human endothelial cells express CCR2 and respond to MCP-1: direct role of MCP-1 in angiogenesis and tumor progression. Blood 2000;96:34–40.
20. Hiratsuka S, Ishibashi S, Tomita T, Watanabe A, Akashi-Takamura S, Murakami M, et al. Primary tumours modulate innate immune signalling to create pre-metastatic vascular hyperpermeability foci. Nat Commun 2013;4:1853.
21. Wessel F, Winderlich M, Holm M, Frye M, Rivera-Galdos R, Vockel M, et al. Leukocyte extravasation and vascular permeability are each controlled in vivo by different tyrosine residues of VE-cadherin. Nat Immunol 2014;15:223–30.
22. Warren NA, Voloudakis G, Yoon Y, Robakis NK, Georgakopoulos A. The product of the gamma-secretase processing of ephrinB2 regulates VE-cadherin complexes and angiogenesis. Cell Mol Life Sci 2018;75:2813–26.
23. Burg N, Swendeman S, Worgall S, Hla T, Salmon JE. Sphingosine -1 Phosphate Receptor-1 signaling maintains endothelial cell barrier function and protects against immune complex-induced vascular injury. Arthritis Rheumatol 2018;70:1879–89.
24. Balkwill FR. The chemokine system and cancer. J Pathol 2012;226:148–57.
25. Willenborg S, Lucas T, van Loo G, Knipper JA, Krieg T, Haase I, et al. CCR2 recruits an inflammatory macrophage subpopulation critical for angiogenesis in tissue repair. Blood 2012;120:613–25.
26. Alva JA, Zovein AC, Monvoisin A, Murphy T, Salazar A, Harvey NL, et al. VE-Cadherin-Cre-recombinase transgenic mouse: a tool for lineage analysis and gene deletion in endothelial cells. Dev Dyn 2006;235:759–67.
27. Winderlich M, Keller L, Cagna G, Broermann A, Kamenyeva O, Kiefer F, et al. VE-PTP controls blood vessel development by balancing Tie-2 activity. J Cell Biol 2009;185:657–71.
28. Sadok A, McCarthy A, Caldwell J, Collins I, Garrett MD, Yeo M, et al. Rho kinase inhibitors block melanoma cell migration and inhibit metastasis. Cancer Res 2015;75:2272–84.
29. Strozyk EA, Desch A, Poeppelmann B, Magnolo N, Wegener J, Huck V, et al. Melanoma-derived IL-1 converts vascular endothelium to a proinflammatory and procoagulatory phenotype via NFkappaB activation. Exp Dermatol 2014;23:670–6.
30. Reichel CA, Khandoga A, Anders HJ, Schlondorff D, Luckow B, Krombach F. Chemokine receptors Ccr1, Ccr2, and Ccr5 mediate neutrophil migration to postischemic tissue. J Leukoc Biol 2006;79:114–22.
31. Schrage A, Loddenkemper C, Erben U, Lauer U, Hausdorf G, Jungblut PR, et al. Murine CD146 is widely expressed on endothelial cells and is recognized by the monoclonal antibody ME-9F1. Histochem Cell Biol 2008;129:441–51.
32. Roblek M, Strutzmann E, Zankl C, Adage T, Heikenwalder M, Atlic A, et al. Targeting of CCL2-CCR2-glycosaminoglycan axis using a CCL2 decoy protein attenuates metastasis through inhibition of tumor cell seeding. Neoplasia 2016;18:49–59.
33. Abraham S, Yeo M, Montero-Balaguer M, Paterson H, Dejana E, Marshall CJ, et al. VE-Cadherin-mediated cell–cell interaction suppresses sprouting via signaling to MLC2 phosphorylation. Curr Biol 2009;19:668–74.
34. Karassek S, Starost L, Solbach J, Greune L, Sano Y, Kanda T, et al. Pertussis toxin exploits specific host cell signaling pathways for promoting invasion and translocation of Escherichia coli K1 RS218 in human brain-derived microvascular endothelial cells. J Biol Chem 2015;290:24835–43.
35. Zhao L, Lim SY, Gordon-Weeks AN, Tapmeier TT, Im JH, Cao Y, et al. Recruitment of a myeloid cell subset (CD11b/Gr1(mid))via CCL2/CCR2 promotes the development of colorectal cancer liver metastasis. Hepatology 2013;57:829–39.
36. Nywening TM, Wang-Gillam A, Sanford DE, Belt BA, Panni RZ, Cusworth BM, et al. Targeting tumour-associated macrophages with CCR2 inhibition in combination with FOLFIRINOX in patients with borderline resectable and locally advanced pancreatic cancer: a single-centre, open-label, dose-finding, non-randomised, phase 1b trial. Lancet Oncol 2016;17:651–62.
37. Roberts TK, Eugenin EA, Lopez L, Romero IA, Weksler BB, Couraud PO, et al. CCL2 disrupts the adherens junction: implications for neuroinflammation. Lab Invest 2012;92:1213–33.
38. Stamatovic SM, Keep RF, Mostarica-Stojkovic M, Andjelkovic AV. CCL2 regulates angiogenesis via activation of Ets-1 transcription factor. J Immunol 2006;177:2651–61.
39. Roodhart JM, He H, Daenen LG, Monvoisin A, Barber CL, van Amersfoort M, et al. Notch1 regulates angio-supportive bone marrow-derived cells in mice: relevance to chemoresistance. Blood 2013;122:143–53.
40. Vestweber D. How leukocytes cross the vascular endothelium. Nat Rev Immunol 2015;15:692–704.

Published OnlineFirst December 14, 2018; DOI: 10.1158/1541-7786.MCR-18-0530

41. Garcia-Roman J, Zentella-Dehesa A. Vascular permeability changes involved in tumor metastasis. Cancer Lett 2013;335:259–69.
42. Vandenbroucke E, Mehta D, Minshall R, Malik AB. Regulation of endothelial junctional permeability. Ann N Y Acad Sci 2008;1123:134–45.
43. Reymond N, d'Agua BB, Ridley AJ. Crossing the endothelial barrier during metastasis. Nat Rev Cancer 2013;13:858–70.
44. Vicente-Manzanares M, Ma X, Adelstein RS, Horwitz AR. Non-muscle myosin II takes centre stage in cell adhesion and migration. Nat Rev Mol Cell Biol 2009;10:778–90.
45. Roblek M, Calin M, Schlesinger M, Stan D, Zeisig R, Simionescu M, et al. Targeted delivery of CCR2 antagonist to activated pulmonary endothelium prevents metastasis. J Control Rel 2015;220:341–7.

Published OnlineFirst December 14, 2018; DOI: 10.1158/1541-7786.MCR-18-0530

Molecular Cancer Research

CCL2 Is a Vascular Permeability Factor Inducing CCR2-Dependent Endothelial Retraction during Lung Metastasis

Marko Roblek, Darya Protsyuk, Paul F. Becker, et al.

Mol Cancer Res 2019;17:783-793. Published OnlineFirst December 14, 2018.